Bayesian Synthetic Likelihood for Calibration of Stochastic Radio Channel Model

Adeogun, Ramoni Ojekunle; Larsen, Claus Meyer; Sand, Dennis; Bovbjerg, Holger Severin; Fisker, Peter Kjær; K. Gjerde, Tor

Published in:
IEEE 94th Vehicular Technology Conference (VTC2021-Fall)

DOI (link to publication from Publisher):
10.1109/VTC2021-Fall52928.2021.9625382

Publication date:
2021

Document Version
Accepted author manuscript, peer reviewed version

Bayesian Synthetic Likelihood for Calibration of Stochastic Radio Channel Model

Ramoni Adeogun, Claus M. Larsen, Dennis Sand, Holger S. Bovbjerg, Peter K. Fisker and Tor K. Gjerde
Department of Electronic Systems, Aalborg University, Aalborg, Denmark,
Email: ra@es.aau.dk; [cmla17,dsand17,hbovbj17,pfiske15,tgjerd20]@student.aau.dk

***Abstract*—This paper presents a novel Bayesian Synthetic Likelihood (BSL) method for calibration of stochastic radio channels without multipath parameter estimation. To calibrate a stochastic channel model, we apply a Markov Chain Monte Carlo (MCMC) algorithm with a Metropolis accept/reject criterion and synthetic likelihood obtained from data generated using the model. The proposed method is applied to calibrate the Turin model and the polarized propagation graph model. Simulation examples show that the BSL method yield similar calibration accuracy to the state-of-the-art method based on Approximate Bayesian Computation (ABC).**

***Index Terms*—Radio propagation, model calibration, Bayesian Synthetic Likelihood, Machine Learning**

I. Introduction

Stochastic radio channel models are useful for the design and analysis of wireless communication systems. This has led to the development of several stochastic models such as Turin [1], Saleh-Valenzuela [2], Extended Saleh-Valenzuela [3], Spencer [4], Propagation Graph (PG) [5], WINNER, and COST. These models require calibration (i.e, estimation of underlying parameters) in order to be useful. Traditionally, the calibration problem is solved using multipath extraction followed by estimation of the model parameters. However, the multipath extraction stage utilizes complex algorithms (such as SAGE [6] and MUSIC [7]), which are prone to errors and difficult to use [8].

Recently, a new paradigm for radio channel model calibration without the complex multipath estimation has been proposed [8], [9]. The existing works are either based on a likelihood-free inference method - Approximate Bayesian Computation (ABC) or function approximation using a Deep Neural Network (DNN) [10]. In [8], a Population Monte Carlo ABC (PMC-ABC) with regression adjustment was used to calibrate the Saleh-Valenzuela (SV) model. On the other hand, a DNN based method was applied to calibrate the SV and propagation graph models in [10]. Both works show reasonable calibration accuracy.

Motivated by the results of recent studies on model parameter estimation using BSL [11], we present the first study on radio channel model calibration via synthetic likelihood (SL) in this paper. SL is a popular method in fields such as economics and biology for performing likelihood-free inference on models with intractable likelihood [12]. We remark here that the SL requires that we are able to simulate from the model to be calibrated for any arbitrary parameter value(s) . Similar to ABC, SL based methods utilize summary statistics from both measured and synthetic data. The synthetic data is generated by sampling the model using some prior on the parameters. In ABC, accept-reject decisions are made based on a distance metric (e.g., Euclidean distance) computed using the measured and simulated statistics. The BSL instead assumes a normal distribution of the summary statistics to compute an auxiliary likelihood of the proposed parameters. Estimates of the model parameters are then obtained by applying standard likelihood based methods on the auxiliary likelihood.

While BSL has been applied successfully for model calibration in other fields, e.g., economics and biology [11], there exist no studies in the open literature on its suitability for calibration of stochastic radio channel models. In this paper, we present the first investigation on application of BSL for estimating the underlying parameters of radio channel models. The main contributions of this work include:

- We propose a method for calibration of radio channel models without multipath extraction based on BSL, Markov Chain Monte Carlo (MCMC) and Metropolis-Hastings criterion. The logarithm of the mean and covariance of the first three temporal moments are used as inputs to the estimator. The proposed method uses the assumption that the summary statistics are normally distributed to obtain an approximation of the likelihood.
- We apply the proposed method to calibrate the Turin model and the propagation graph (PG) model.
- We perform simulations to evaluate performance of the BSL based approach and compare to existing approaches based on PMC - ABC.

II. BSL for Calibration

Given a stochastic radio channel model, $\mathcal{M}(\boldsymbol{\theta})$, the goal of calibration is to fit the model to a set of measured data, $\mathbf{y} \in \mathbb{R}^n$. This corresponds to estimating a $p-$dimensional parameter vector, $\boldsymbol{\theta}$ from the measurement data. Similar to the ABC method in [8], the BSL relies on summarizing $\mathbf{y}$ into a low-dimensional vector of summaries, $\mathbf{s}_y : \mathbb{R}^n \to \mathbb{R}^d$, which are informative about $\boldsymbol{\theta}$. In BSL, the goal is to use the summary statistic, $\mathbf{s}_y$ for simulating the posterior distribution given as

$$p(\boldsymbol{\theta}|\mathbf{s}_\mathbf{y}) \propto p(\mathbf{s}_\mathbf{y}|\boldsymbol{\theta})p(\boldsymbol{\theta}) \tag{1}$$

where $p(\boldsymbol{\theta})$ is the prior distribution. Since most radio channels are typically complex, the likelihood may easily become analytically intractable. We instead use synthetic likelihood

(SL) [12] to approximate (1). As in [11], the SL involves approximating $p(\mathbf{s_y}|\boldsymbol{\theta})$ as a multivariate normal distribution, i.e.,

$$p(\mathbf{s_y}|\boldsymbol{\theta}) \approx \mathcal{N}(\boldsymbol{\mu_\theta}, \boldsymbol{\Sigma_\theta}), \tag{2}$$

where $\boldsymbol{\mu_\theta}$ and $\boldsymbol{\Sigma_\theta}$ denote the mean vector and covariance matrix, respectively. Using the probability distribution function of a multivariate normal distribution, the log-likelihood can be expressed as

$$\ln\left(p(\mathbf{s_y}|\boldsymbol{\theta})\right) = -\frac{1}{2}(\mathbf{s_y} - \boldsymbol{\mu_\theta})^T \boldsymbol{\Sigma_\theta}^{-1}(\mathbf{s_y} - \boldsymbol{\mu_\theta}) - \frac{1}{2}\ln|\boldsymbol{\Sigma_\theta}|, \tag{3}$$

where $|\mathbf{A}|$ denotes the determinant of $\mathbf{A}$. To estimate the mean and covariance, multiple independent realisations are drawn from the model at $\boldsymbol{\theta}$. The resulting realisations are then reduced to summary statistics. The simulated summaries are used to compute unbiased estimates of $\boldsymbol{\mu}$ and $\boldsymbol{\Sigma}$ as

$$\hat{\boldsymbol{\mu}}_{\boldsymbol{\theta}} = \frac{1}{L}\sum_{\ell=1}^{L}\mathbf{s}_\ell$$

$$\hat{\boldsymbol{\Sigma}}_{\boldsymbol{\theta}} = \frac{1}{L-1}\sum_{\ell=1}^{L}(\mathbf{s}_\ell - \boldsymbol{\mu_\theta})(\mathbf{s}_\ell - \boldsymbol{\mu_\theta})^T \tag{4}$$

where $\mathbf{s}_\ell$ is the ℓth simulated summary statistic vector, and L is the total number of simulated summary statistic vectors.

Using the SL obtained by substituting the estimates in (4) into (3), it is now possible to use likelihood-based inference methods to estimate the posterior distribution. This can be done using the Markov Chain Monte Carlo (MCMC) method [13] to sample the posterior distribution. We chose the Metropolis algorithm [13] in this work. Thus, a proposed parameter vector, $\boldsymbol{\theta}^*$ at sampling instant, i is accepted with probability $\exp(p(\mathbf{s_y}|\boldsymbol{\theta}^*) - p(\mathbf{s_y}|\boldsymbol{\theta}^{i-1}))$.

This combination of the well-known Metropolis algorithm and the synthetic likelihood method is referred to as MCMC - BSL. An algorithmic description of the MCMC - BSL method for calibration is shown in 1. Since the Metropolis algorithm requires a symmetric proposal distribution, $q(\boldsymbol{\theta})$, we use a multivariate normal distribution centered around the last accepted step.

Algorithm 1: MCMC BSL for Calibration of Stochastic Channel Models.

Input: Prior distribution $p(\boldsymbol{\theta})$, observed summary statistics $\mathbf{s_y}$, number of model realisations for summary statistic computation, N_r, number of summary statistics vectors used per likelihood, L, number of MCMC steps, K
Output: Approximate posterior distribution of $\boldsymbol{\theta}$

```
Draw θ^0 from the prior distribution;
for j = 1 to L do
    Draw N_r model realisations using θ^0;
    Calculate a summary statistics vector s*_j;
end
Calculate log-likelihood, p(s_y|θ^0) using (3);
for i = 1 to K − 1 do
    Draw θ* from proposal distribution N(θ^{i−1}, Σ_θ);
    for j = 1 to L do
        Draw N_r model realisations using θ*;
        Calculate a summary statistics vector s*_j;
    end
    Calculate log-likelihood, p(s_y|θ*) using (3);
    Compute r = exp(p(s_y|θ*) − p(s_y|θ^{i−1}));
    if U(0, 1) < r then
        θ^i = θ*;
    else
        θ^i = θ^{i−1};
    end
end
```

III. Application to Stochastic Channel Models

We apply the proposed calibration method to calibrate two stochastic channel models viz: the stochastic polarized propagation graph model (SPPGM) [14] and the Turin Model (TM) [1]. The measurement model, choice of summary statistics and the channel models are described in this section.

A. Measurement Model

We consider a linear, time-invariant single input single output (SISO) radio channel and measurement data collected using a vector network analyzer (VNA) with bandwidth B. The measured signal at each frequency point can be expressed as

$$Y[k] = H[k] + N[k], \quad k = 0, 1, \cdots, K-1, \tag{5}$$

where $H[k]$ denotes the transfer function measured at K equidistant frequency points with a separation of $\Delta f = B/(K-1)$. $N[k]$ is the measurement noise assumed for each k to be independent and identically distributed (iid) circular complex Gaussian with variance σ^2. By taking the discrete-frequency, continuous-time inverse Fourier transform of (5), we obtain the measured signal in time-domain

$$y(t) = \frac{1}{K}\sum_{k=0}^{K-1} Y[k]\exp(j2\pi k\Delta f t), \tag{6}$$

which is periodic with period $t_{\max} = 1/\Delta f$. Since the number of measurement points is typically large (i.e., in the order of hundreds or thousands), we summarize the measured data into its first V temporal moments, defined as

$$m_v = \int_0^{t_{\max}} t^v |y(t)|^2 \mathrm{d}t, \quad v = 0, 1, 2, \ldots, (V-1). \tag{7}$$

With (7), the measured data is compressed into a $K \times V$ matrix of temporal moments. Depending on the bandwidth and sampling rate, the number of delay points K and hence the matrix of temporal moments may also be large. We therefore resort to the mean and covariance of the temporal moments as summary statistics for calibrating the model. To satisfy the BSL's normal distribution assumption, we further compute the natural logarithm of the summary statistics. Note that the temporal moments have been shown in [15] to be lognormal distributed.

B. Turin Model

Consider the multipath propagation model defined as

$$H[k] = \sum_{l=0}^{\infty} \alpha_l \cdot \exp(-\mathrm{j}2\pi k \tau_l \Delta f) \tag{8}$$

where l is the multipath component number, α_l is the complex gain, τ_l is the time delay of the l'th multipath component and Δf is the frequency separation. In the Turin model [1], α and τ form a marked Poisson point process with points τ, marks α and intensity λ. The complex gain α can be modelled as a zero mean complex Gaussian with variance $\sigma_\alpha^2(t)$. The time delays τ are modelled as a homogeneous Poisson point process with arrival rate λ. This process has the power delay profile $P_h(t) = \lambda \cdot \sigma_\alpha^2(t)$.

In general the in-room power delay profile is a decaying function of time and can be approximated by the reverberation model [16]

$$P_h(t) = \begin{cases} G_0 \cdot \exp(\frac{-t}{T}) & t \geq t_0 \\ 0 & \text{otherwise} \end{cases} \tag{9}$$

where G_0 is the gain at zero delay, T is reverberation time, t is the time in seconds and t_0 is the delay of the first multipath component. Calibration of the Turin model therefore requires estimating the parameter vector, $\boldsymbol{\theta} = [G_0, T, \lambda, \sigma^2]$.

C. Polarized Propagation Graph Model

In the stochastic polarized propagation graph model (SPPGM) [14], [17], [18], the channel is represented as a propagation graph [5] with the transmitters, the receivers, and the scatterers as vertices. Consider a wireless system with N_r receivers, and N_t transmitters in an environment with N_s scatterers. The transfer function matrix at a frequency point, k, $\mathbf{H}[k]$ from the PG model, is defined as

$$\mathbf{H}[k] = \mathbf{D}[k] + \mathbf{R}[k][\mathbf{I} - \mathbf{B}[k]]^{-1}\mathbf{T}[k], \tag{10}$$

where $\mathbf{D}[k] \in \mathbb{C}^{N_\mathrm{r} \times N_\mathrm{t}}$, $\mathbf{T}[k] \in \mathbb{C}^{2N_\mathrm{s} \times N_\mathrm{t}}$, $\mathbf{R}[k] \in \mathbb{C}^{N_\mathrm{r} \times 2N_\mathrm{s}}$ and $\mathbf{B}[k] \in \mathbb{C}^{2N_\mathrm{s} \times 2N_\mathrm{s}}$ denote the direct transmitter to receiver, transmitter to scatterer, scatterer to receiver, and scatterer to scatterer edge transfer function sub-matrices, respectively. The transfer function sub-matrices are given as

$$\begin{aligned} \mathbf{D}[k] &= \mathcal{X}_\mathrm{t}^T(\Omega_e)\mathcal{X}_\mathrm{r}(\Omega_e)G_e[k], \quad e \in \mathcal{E}_\mathrm{d} \\ \mathbf{T}[k] &= \mathcal{X}_\mathrm{t}^T(\Omega_e)\mathbf{M}\boldsymbol{\Gamma}(\Omega_e)G_e[k], \quad e \in \mathcal{E}_\mathrm{t} \\ \mathbf{B}[k] &= \mathbf{M}\boldsymbol{\Gamma}(\Omega_e)G_e[k], \quad e \in \mathcal{E}_\mathrm{s} \\ \mathbf{R}[k] &= \mathcal{X}_\mathrm{r}(\Omega_e)G_e[k], \quad e \in \mathcal{E}_\mathrm{r}, \end{aligned} \tag{11}$$

where Ω_e denotes the direction of propagation, $\mathcal{X}_\mathrm{t}(\Omega_e)$ and $\mathcal{X}_\mathrm{r}(\Omega_e)$ are the 2×1 transmit and receive polarimetric antenna array response vectors, respectively, and $\boldsymbol{\Gamma}(\Omega_e)$ is the 2×2 rotation matrix. The 2×2 coupling between the two polarization states, $\mathbf{M}$ is defined as [14]

$$\mathbf{M} = \frac{1}{1+\gamma}\begin{bmatrix} 1 & \gamma \\ \gamma & 1 \end{bmatrix}, \tag{12}$$

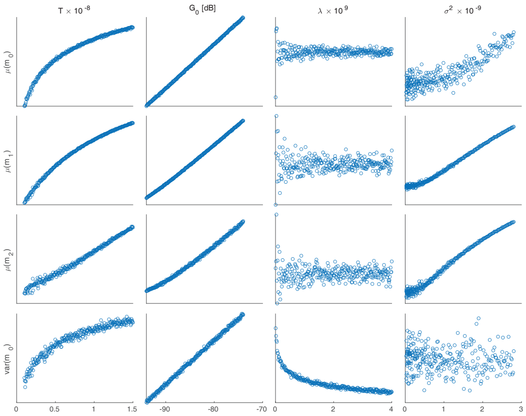

Fig. 1. Comparison of summary statistics versus varying parameter values.

where $\gamma \in (0, 1)$ is the polarisation power coupling ratio. In (11), $G_e[k]$ accounts for the polarisation-independent propagation characteristics, and is expressed as

$$G_e[k] = g_e[k] \exp[j(\psi_e - 2\pi k \tau_e \Delta f)], \tag{13}$$

where ψ_e is the phase assumed to be uniformly distributed between 0 and 2π. The edge gain, $g_e[k]$ is defined as

$$g_e[k] = \begin{cases} \frac{1}{(4\pi k \Delta f \tau_e)}; & e \in \mathcal{E}_\mathrm{d} \\ \frac{1}{\sqrt{4\pi\tau_e^2 k \Delta f \mu(\mathcal{E}_\mathrm{t}) \mathcal{S}(\mathcal{E}_\mathrm{t})}}; & e \in \mathcal{E}_\mathrm{t} \\ \frac{g}{\mathrm{odi}(e)}; & e \in \mathcal{E}_\mathrm{s} \\ \frac{1}{\sqrt{4\pi\tau_e^2 k \Delta f \mu(\mathcal{E}_\mathrm{r}) \mathcal{S}(\mathcal{E}_\mathrm{r})}}; & e \in \mathcal{E}_\mathrm{r} \end{cases} \tag{14}$$

where $g \in (0, 1)$ denote the reflection gain, $\mathrm{odi}(e)$ denotes the number of outgoing edges from the n^{th} scatterer, and

$$\mu(\mathcal{E}_\mathrm{a}) = \frac{1}{|\mathcal{E}_\mathrm{a}|}\sum_{e \subset \mathcal{E}_\mathrm{a}} \tau_e, \quad \mathcal{S}(\mathcal{E}_\mathrm{a}) = \sum_{e \subset \mathcal{E}_\mathrm{a}} \tau_e^{-2}, \quad \mathcal{E}_\mathrm{a} \subset \mathcal{E},$$

with $|\cdot|$ denoting cardinality of the associated set.

To draw a random graph and simulate the transfer function from the model, we need to specify values of g, N_s and γ as well as the transceiver positions. Scatterers are placed across the floor of the room with uniform distribution. Edges in the graph are then drawn randomly depending on P_vis. The edge weights and sub-matrices are calculated using (11) – (14) and the transfer matrices using (10). The implementation used in this paper assumes omnidirectional antennas at both the transmitter and receiver. To calibrate the PPGM, we estimate the 5-dimensional parameter vector $\boldsymbol{\theta} = [g, N_\mathrm{s}, P_\mathrm{vis}, \gamma, \sigma^2]$ from data.

IV. Numerical simulations and results

We apply the BSL method to calibrate the models described in Section III using the summary statistics presented in this same section. The algorithm is compared with the PMC-ABC method in [9]. The two methods are evaluated via simulations. For the SPPGM, we compare with the performance results of the PMC-ABC calibration method presented in [9].

TABLE I
SUMMARY OF PRIOR RANGES AND PARAMETER ESTIMATES

Model	Parameter	Prior range	Estimate (standard deviation) Simulated data		
	θ		**True value**	**BSL**	**ABC**
Turin	Reverberation time, T [s]	$[10^{-9},\ 15\cdot10^{-9}]$	$7.8\cdot10^{-9}$	$7.96\cdot10^{-9}\ (2.19\cdot10^{-10})$	$7.56\cdot10^{-9}\ (1.44\cdot10^{-9})$
	Initial gain, G_0	$[-94\,\mathrm{dB},\ -74\,\mathrm{dB}]$	$-83{,}9\,\mathrm{dB}$	$-83{,}94\,\mathrm{dB}\ (0{,}27\,\mathrm{dB})$	$-82{,}99\,\mathrm{dB}\ (1{,}9\,\mathrm{dB})$
	Ray arrival rate, λ [Hz]	$[5\cdot10^{6},\ 4\cdot10^{9}]$	$1\cdot10^{9}$	$1.023\cdot10^{9}\ (9.50\cdot10^{7})$	$1.98\cdot10^{9}\ (1.06\cdot10^{9})$
	Noise variance, σ_{N}^2	$[2.8\cdot10^{-11},\ 2.8\cdot10^{-9}]$	$0.28\cdot10^{-9}$	$0.287\cdot10^{-9}\ (5.55\cdot10^{-7})$	$0.25\cdot10^{-9}\ (6.64\cdot10^{-6})$
SPPGM	Reflection gain, g	[0, 1]	0.65	0.66 (0.025)	0.64 (0.110)
	Number of scatterer, N	[5, 50]	15	15 (1.586)	15 (3.01)
	Prob. of visibility, P_{vis}	[0, 1]	0.9	0.90 (0.029)	0.910 (0.025)
	Polarization ratio, γ	[0, 1]	0.1	0.107 (0.011)	0.096 (0.063)
	Noise variance, σ^2	$[2\cdot10^{-10}, 2\cdot10^{-9}]$	10^{-9}	$1.01\cdot10^{-9}(3.824\cdot10^{-13})$	$1.13\cdot10^{-9}(7\cdot10^{-12})$

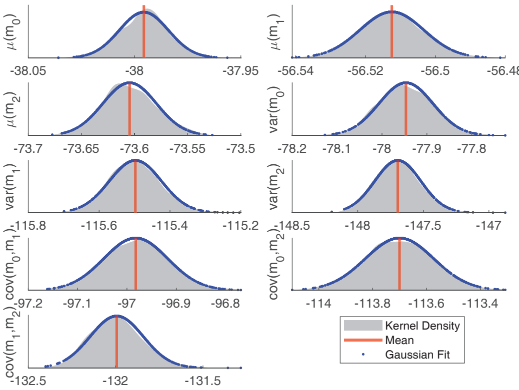

Fig. 2. Gaussian fit to summary statistics computed using the Turin model. Similar results were obtained for the PG model.

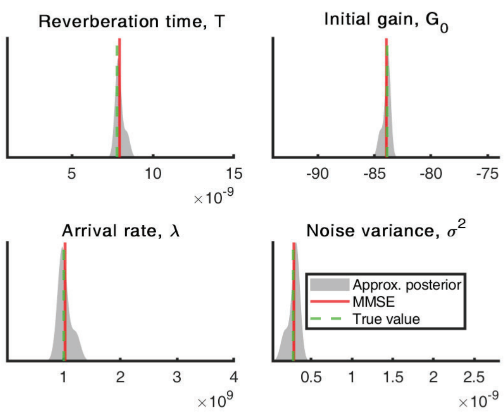

Fig. 3. Kernel density estimate of the posterior distribution of the Turin model parameters obtained from BSL.

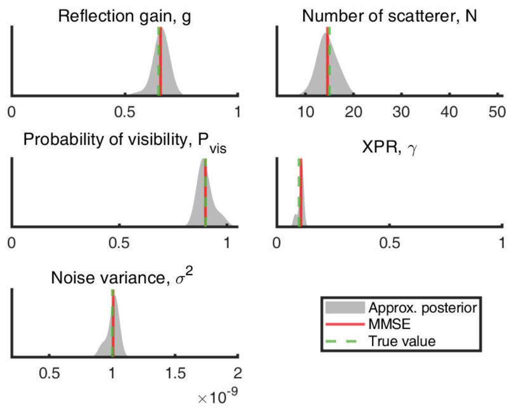

Fig. 4. Kernel density estimate of the posterior distribution of propagation graph model parameters obtained from BSL.

In the simulations, we set some *true* values, $\boldsymbol{\theta}_{\mathbf{true}}$ for the parameters of the models. The observed data is then generated by sampling from the models at $\boldsymbol{\theta}_{\mathbf{true}}$. The true parameters for the SPPGM and Turin model are set based on those in [9] and [19], respectively. The parameters are shown in Table I. We consider an in-room environment with dimension $4\ \mathrm{m}\times 4\ \mathrm{m}\times 3\ \mathrm{m}$ for the SPPGM.

For each model, we draw 300 realisations of the channel with the specified true parameters. The generated channel responses were then converted into summary statistics following the procedure described in Section III. We denote the summary statistics corresponding to $\boldsymbol{\theta}_{\mathbf{true}}$ as s_{obs}. Based on the observations in previous studies [8]–[10], we additionally use the cross-polarization ratio (XPR), defined as the ratio of the averaged power of the co-polarized to the cross-polarized channel as a summary statistic. Thus, s_{obs} has dimensions 9×1 and 10×1 for the Turin and SPPGM, respectively.

A. Properties of summary statistics

We attempt to answer two questions viz: *Are the selected summary statistics informative about the model parameters?* and *Are the summary statistics marginally and jointly Gaussian?*. While the former determines how well the model parameters can be estimated, the latter is a necessary requirement for the application of BSL.

In Fig. 1, we show the variation of the first four summary statistics with changes in each parameter of the Turin model. The figures show that the summary statistics are quite informative about individual parameters. The other five summary statistics showed similar trend but are not shown in due to space constraint. Based on the trends in this figure and observations in existing works applying ABC, we conclude that the

BSL should be able to accurately estimate the parameters of the model using the selected statistics. We remark here that similar analysis have been presented in [9] for the SPPGM.

To answer the second question, we show the kernel density estimates of the marginal probability distributions and Gaussian fits to the summary statistics obtained from the Turin model, in Fig. 2. We observe that the density estimates and corresponding Gaussian fits are very similar indicating that the statistics are marginally Gaussian. Based on this observation and the results in [15], we conclude that the chosen summary statistics are jointly normal and hence, the BSL algorithm can be applied to calibrate the Turin model. Similar results were obtained for the SPPGM. These are not shown here due to space constraints and the high similarity between the figures.

B. Results

We evaluate the proposed MCMC BSL by applying it to calibrate the Turin model and the SPPGM using synthetic data. The goal is to obtain the approximate posterior distributions of the parameters as well as point estimates of the true parameters. Similar to [9], a uniform prior over the ranges specified in Table I is used for all model parameters. During the simulations, we compute the summary statistics using 300 model realization. The likelihood is then estimated using 50 summary statistics vectors. A total of 2000 MCMC steps were performed out of which the last 200 is used as the accepted samples.

In Fig. 3 and Fig. 4, we show the kernel density estimates of the accepted BSL samples as approximations of the posterior distribution of the parameters of Turing model and the SPPGM, respectively. The MMSE estimates and the corresponding true values are also shown in the figures. The figures show that the estimated parameters for both models are very accurate with insignificant deviation from the true values. The figures also show very narrow posterior density estimates for all parameters translating to small standard deviations as shown in Table. I. The approximate posteriors in Fig. 3 and Fig. 4 compare reasonably well with those obtained from the application of ABC in [19] and [9], respectively. As shown in Table I, the MCMC-BSL calibration method appear to yield slightly better MMSE estimates and lower standard deviations than the ABC[1] for some of the parameters. As indicated in [12], the gain from using BSL over ABC may become pronounced for complex models requiring high dimensional summary statistics.

V. Conclusion

In this paper a BSL method for calibration of stochastic radio channel models is proposed, and has been used to successfully calibrate the Turin model and the stochastic polarized propagation graph model (SPPGM) using the MCMC algorithm with Metropolis accept-reject criterion. It is observed that the selected summary statistics are normally distributed with adequate information about parameters of the models. For both models, the BSL shows comparable performance with existing methods based on PMC-ABC.

[1]The reported estimates and standard deviations are based on application of PMC-ABC [9] to the Turin. For the SPPGM, the estimates are those reported in [9].

References

[1] G. L. Turin, F. D. Clapp, T. L. Johnston, S. B. Fine, and D. Lavry, "A statistical model of urban multipath propagation channel," *IEEE Transactions on Vehicular Technology*, vol. 21, no. 1, pp. 1–9, 2 1972.

[2] A. A. M. Saleh and R. A. Valenzuela, "A statistical model for indoor multipath propagation," *IEEE Journal on Selected Areas in Communications*, vol. 5-SAC, no. 2, pp. 128–137, 2 1987.

[3] C. Gustafson, K. Haneda, S. Wyne, and F. Tufvesson, "On mm-wave multipath clustering and channel modeling," *IEEE Transactions on Antennas and Propagation*, vol. 62, no. 3, pp. 1445–1455, 2013.

[4] Q. H. Spencer, B. D. Jeffs, M. A. Jensen, and A. L. Swindlehurst, "Modeling the statistical time and angle of arrival characteristics of an indoor multipath channel," *IEEE Journal on Selected Areas in Communications*, no. 3, pp. 347–360, 3 2000.

[5] T. Pedersen, G. Steinböck, and B. H. Fleury, "Modeling of reverberant radio channels using propagation graphs," *IEEE Trans. Antennas Propag.*, vol. 60, no. 12, pp. 5978–5988, Dec 2012.

[6] B. H. Fleury, M. Tschudin, R. Heddergott, D. Dahlhaus, and K. I. Pedersen, "Channel parameter estimation in mobile radio environments using the sage algorithm," *IEEE Journal on Selected Areas in Communications*, vol. 17, no. 3, pp. 434–450, 1999.

[7] R. Schmidt, "Multiple emitter location and signal parameter estimation," *IEEE Transactions on Antennas and Propagation*, vol. 34, no. 3, pp. 276–280, 1986.

[8] A. Bharti and T. Pedersen, "Calibration of stochastic channel models using approximate bayesian computation," in *IEEE GLOBECOM Workshops*. IEEE, 2019.

[9] A. Bharti, R. O. Adeogun, and T. Pedersen, "Learning parameters of stochastic radio channel models from summaries," *IEEE Open Journal of Antennas and Propagation*, vol. 1, pp. 175–188, May 2020.

[10] R. Adeogun, "Calibration of stochastic radio propagation models using machine learning," *IEEE Antennas and Wireless Propagation Letters*, vol. 18, pp. 2538–2542, 12 2019.

[11] S. N. Wood, "Statistical inference for noisy nonlinear ecological dynamic systems," *Nature*, vol. 466, pp. 1102–1107, Aug. 2010.

[12] L. F. Price, C. C. Drovandi, A. Lee, and D. J. Nott, "Bayesian synthetic likelihood," *Journal of Computational and Graphical Statistics*, vol. 27, no. 1, pp. 1–11, 2018.

[13] A. Gelman, J. Carlin, H. Stern, D. Dunson, A. Vehtari, and D. Rubin, *Bayesian Data Analysis, Third Edition*, ser. Chapman & Hall/CRC Texts in Statistical Science. Taylor & Francis, 2013.

[14] R. Adeogun, T. Pedersen, C. Gustafson, and F. Tufvesson, "Polarimetric Wireless Indoor Channel Modelling Based on Propagation Graph," *IEEE Transactions on Antennas and Propagation*, vol. 67, no. 10, pp. 6585–6595, oct 2019.

[15] A. Bharti, R. Adeogun, X. Cai, W. Fan, F.-X. Briol, L. Clavier, and T. Pedersen, "Joint modeling of received power, mean delay, and delay spread for wideband radio channels," *IEEE Transactions on Antennas and Propagation*, 2021.

[16] G. Steinböck, T. Pedersen, B. H. Fleury, W. Wang, and R. Raulefs, "Distance dependent model for the delay power spectrum of in-room radio channels," *IEEE Transactions on Antennas and Propagation*, vol. 61, no. 8, pp. 4327–4340, 2013.

[17] R. O. Adeogun, A. Bharti, and T. Pedersen, "An iterative transfer matrix computation method for propagation graphs in multi-room environments," *IEEE Antennas and Wireless Propagation Letters*, vol. 18, no. 4, pp. 616–620, April 2019.

[18] R. Adeogun and T. Pedersen, "Propagation graph based model for multipolarized wireless channels," in *IEEE WCNC*, April 2018.

[19] A. Bharti, R. Adeogun, and T. Pedersen, "Parameter estimation for stochastic channel models using temporal moments," in *2019 IEEE International Symposium on Antennas and Propagation and USNC-URSI Radio Science Meeting*, ser. IEEE Antennas and Propagation Society. International Symposium. IEEE, Oct. 2019, pp. 1267–1268.